Influence of Alloying Elements on the Corrosion Performance of Alloy 33 and Alloy 24 in Seawater

G. Latha, N. Rajendran, and S. Rajeswari

The nitrogen-bearing alloys (alloy 33 and alloy 24) and stainless steel type 316L were used in this investigation in order to study the effect of alloying elements on electrochemical behavior and on the nature of passive film in seawater. Scanning electron microscopic studies were carried out to identify the pit morphology of the alloys. Surface analysis of the alloys by x-ray photoelectron spectroscopy after passivation showed that nitrogen and chromium are enriched at the surface of the passive film.

Keywords alloy 24, alloy 33, passive film, scanning electron microscopy, x-ray photoelectron spectroscopy

1. Introduction

A great deal of effort has been spent on the development of alloys that exhibit higher corrosion resistance in seawater. The commonly used metals span a wide spectrum, starting from carbon steel to high-performance nickel-base alloys. Even though the standard austenitic stainless steels have been and continue to be the most frequently selected materials for use in marine-related components, their vulnerability to localized corrosion—mainly due to pitting and crevice attack—has been a major problem (Ref 1-3). Earlier reports on the beneficial effects of nickel, chromium, molybdenum, and nitrogen contents in improving the localized corrosion resistance have led to the development of different alloys with varying composition (Ref 4-8). More recently, life-cycle costs together with the identification of preferably less costly alloying additions are being considered to enhance the corrosion resistance of the material. Alloy 33 (UNS R20033) and alloy 24 (UNS S34565) contain substantially higher amounts of alloying elements, namely, chromium, molybdenum, and nitrogen, and their cost effectiveness is comparable to the nickel-base alloys.

The present work was undertaken to study the localized corrosion behavior of the alloys by the polarization method. Scanning electron microscopy (SEM) studies were performed to identify the pit morphology of the alloys. X-ray photoelectron spectroscopy (XPS) studies were undertaken to identify the elements present in the passive film and to elucidate the chemical state of the elements present in the surface and inside the passive film by electron sputtering.

G. Latha, N. Rajendran, and **S. Rajeswari,** Department of Analytical Chemistry, University of Madras, Guindy Campus, Madras 600 025, India.

2. Experimental Procedure

2.1 *Polarization Studies*

The electrochemical cell consists of three compartments with a capacity of 500 mL. Saturated calomel electrode was used as the reference electrode, platinum foil as the counter, and the test alloys (stainless steel alloy 316L, alloy 33, and alloy 24) as the working electrode. Natural seawater was used as the electrolyte.

The working electrode was prepared by cutting the alloys (chemical composition of the alloys are given in Table 1) into $1 \times 1 \times 0.3$ cm samples. Each piece was attached with a brass rod using silver paste for electrical contact. Then the samples were molded in epoxy resin such that an area of 1 cm^2 was exposed. The mounted samples were successively polished using grit papers, and final polishing was done using diamond paste in order to obtain a scratch-free mirror finish. The electrodes were ultrasonically cleaned with soap solution, degreased using acetone, and thoroughly rinsed in distilled water and dried. Identical procedure was followed for all the electrodes to minimize any experimental fluctuations.

During the potentiodynamic anodic cyclic polarization studies, the electrode was allowed to stabilize for 30 min. After attaining the stable corrosion potential (E_c), the potential was scanned at a step of 1 mV/s applied to the working electrode with respect to the reference electrode until the current raised abruptly. The corresponding potential is termed the critical pitting potential (E_b), where the alloy entered the transpassive region or pitted. The sweep direction was then reversed after reaching an anodic current density of 3 mA/cm^2 until the potential where the reverse scan meets the passive region. This potential is termed the pit-repassivation potential (E_p).

Evaluation of the corrosion resistance of an alloy is usually determined by measuring the pitting and repassivation potential, and hence these parameters were recorded after each polarization study. Triplicate polarization experiments were conducted to get precise values of pitting and repassivation potentials.

Table 1 Chemical composition of 316L SS, alloy 33, and alloy 24

Alloy	Composition, wt%								
	Cr	Ni	Mn	Si	Mo	C	N	S	Fe
316L SS	17.20	12.60	1.95	0.003	2.40	0.030	0.02	0.030	Bal
Alloy 33	32.85	30.95	0.64	0.310	1.67	0.007	0.39	0.004	Bal
Alloy 24	24.20	17.70	6.14	0.030	4.34	0.012	0.46	0.004	Bal

2.2 *Scanning Electron Microscopy Studies*

Scanning electron microscopy studies were undertaken to identify the pit morphology of the alloys. The alloys were polarized slightly above the pitting potential, removed from the cell, rinsed with water, cleaned with acetone, dried, and examined by SEM.

2.3 *X-Ray Photoelectron Spectroscopy Measurements*

X-ray photoelectron spectroscopy studies were performed to characterize the passive film on alloy 33 and alloy 24. The working electrodes were anodically polarized at 200 mV in seawater for a period of 1 h for the growth of the passive film. Then the samples were removed from the polarization cell assembly, rinsed with triply distilled water, dried in a stream of flowing argon, and kept inside a desiccator until they were transferred to the evacuated sample chamber of the electron spectrometer for chemical analysis (ESCA). The operating pressure was maintained between 10^{-8} to 10^{-9} torr. The XPS analysis was run with Al Kα source with a mean kinetic energy of 1486.6 eV. The spectrum of the material was surveyed first. This was followed by a detailed examination of the individual spectra of carbon (1*s*), nitrogen (1*s*), chromium (2*p*), and molybdenum (3*d*) peaks.

The binding energy of the alloying elements were measured from the spectra obtained for the respective elements, and the values were energy corrected with respect to the reference carbon (1*s*) binding energy value. The area under the peaks obtained for iron and chromium was taken into account to calculate the peak area ratios.

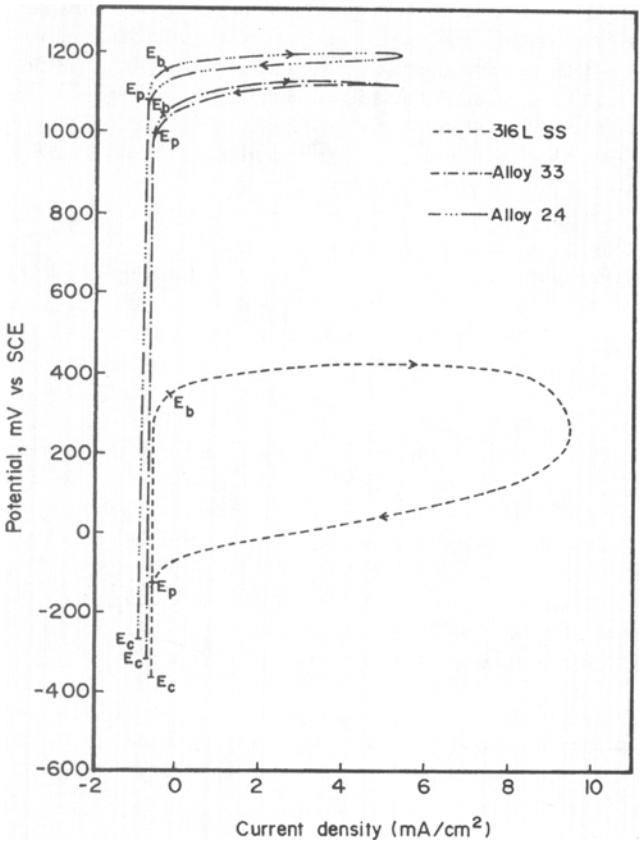

Fig. 1 Potentiodynamic anodic cyclic polarization performance of the alloys in seawater

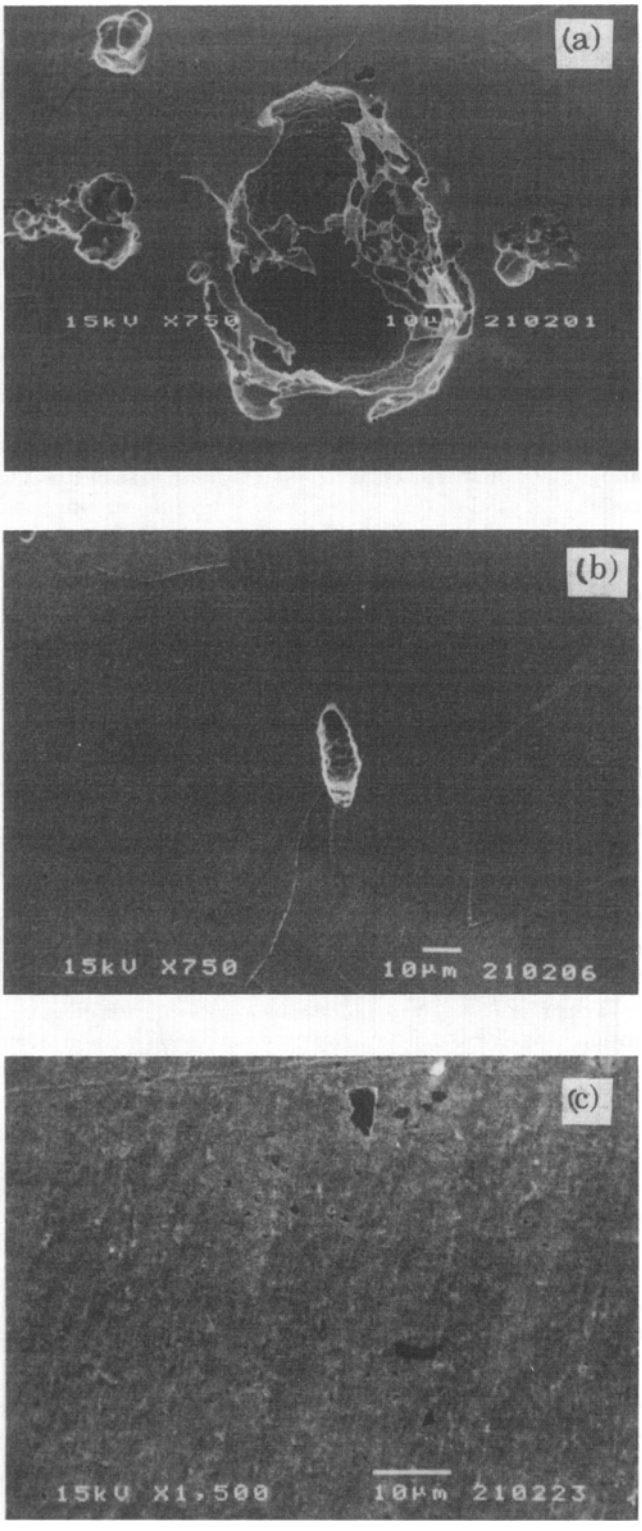

Fig. 2 Scanning electron micrographs showing pit morphology of alloys (a) 316L SS, (b) alloy 33, and (c) alloy 24

3. Results and Discussion

3.1 *Corrosion Studies*

The pitting corrosion behavior of stainless steel type 316L (SS), alloy 33, and alloy 24 are shown in Fig. 1. From the cyclic polarization curves, the parameters recorded were the corrosion potential (E_c), the pitting potential (E_b), and the repassivation potential (E_p).

All of the alloys exhibited a passive region right from the corrosion potential onward. However, the passive region was very much smaller for 316L SS compared to alloy 33 and alloy 24. The pitting potential of 365 mV was observed for 316L SS, whereas for alloy 33 and alloy 24 it was shifted toward the more noble direction. The pitting potential is considered to be the criterion for evaluating the pitting corrosion resistance of the materials that is directly influenced by the amount of passivating elements present in the alloy (Ref 3, 5). The presence of higher amounts of chromium, nitrogen, and molybdenum in alloy 33 and alloy 24 compared to that of 316L SS would certainly inhibit the pit initiation and pit growth kinetics.

3.2 *Scanning Electron Microscopy Studies*

The scanning electron micrographs of the alloys after the pitting are shown in Fig. 2(a to c). The pit morphology of 316L SS shows spherical and larger pits (~100 μm) across, whereas alloy 33 and alloy 24 exhibited very small pits (~10 μm). This indicates that the alloying elements (mainly, chromium and nitrogen in alloy 33 and alloy 24) decrease the aggressiveness of the local pit sites and hence prevent the growth of the pits.

3.3 *Analysis of the Passive Film by XPS*

3.3.1 Chromium ($2p_{3/2}$) Spectra

In the case of alloy 316L, two peaks were deconvoluted at the binding energy values of 576.3 and 578.1 eV before sputtering the passive film. After sputtering, a peak at 574.1 eV was identified along with the peaks at 576.3 and 578.1 eV (Fig. 3). For alloy 33 and alloy 24, three peaks were observed at the binding energy values of 576.3, 576.7, and 578.1 eV before sputtering the passive film. After sputtering the passive film, two peaks were observed at 574.1 and 579.1 eV along with the peaks at 576.3 and 578.1 eV.

On the basis of the previously reported results (Ref 9-12), the binding energy values 574.1, 576.3, and 578.1 eV correspond to the presence of chromium in the form of Cr (metallic), Cr^{3+}, and Cr^{6+}. The peaks at 576.7 and 579.1 eV indicate the presence of chromium in the form of CrOOH and CrO_4^{2-} (Ref 10, 13).

In all of the above alloys, chromium was found in the form of oxides such as Cr_2O_3 and CrO_3, respectively. This result is in accordance with earlier reports (Ref 9-13). Besides, the presence of CrOOH at 576.7 eV and CrO_4^{2-} at 579.1 eV was observed in alloy 33 and alloy 24.

3.3.2 Molybdenum ($3d_{5/2}$) Spectra

The specimens were scanned between the binding energy ranging between 225.0 and 235.0 eV to identify the presence of molybdenum. Four peaks were deconvoluted from the peak obtained for alloy 316L corresponding to the binding energy values of 228.3, 229.2, 230.7, and 232.2 eV. After sputtering the passive film, the peak at 228.3 eV was not observed, whereas the remaining peaks were present besides the peak at 227.2 eV (Fig. 4).

In the case of alloy 33 and alloy 24, similar peaks at the binding energy values of 228.3, 229.3, 230.7, and 232.2 eV corresponding to molybdenum in the form of Mo^{3+}, Mo^{4+}, Mo^{5+}, and Mo^{6+} were observed. In addition, the peak at 227.2 eV was observed in the case of alloy 24, which is due to the presence of molybdenum in the metallic state. The presence of Mo^{6+} contribution dominates compared to the 316L. Of particular interest is the steeper slope of the molybdenum content, which indicates the higher surface content of Mo^{6+} in alloy 24 compared to alloy 33. After sputtering alloy 24, the peak corresponding to metallic Mo, Mo^{4+}, Mo^{5+}, and Mo^{6+} were found, whereas Mo^{3+} was not. However, in alloy 33 neither metallic Mo nor Mo^{3+} was found.

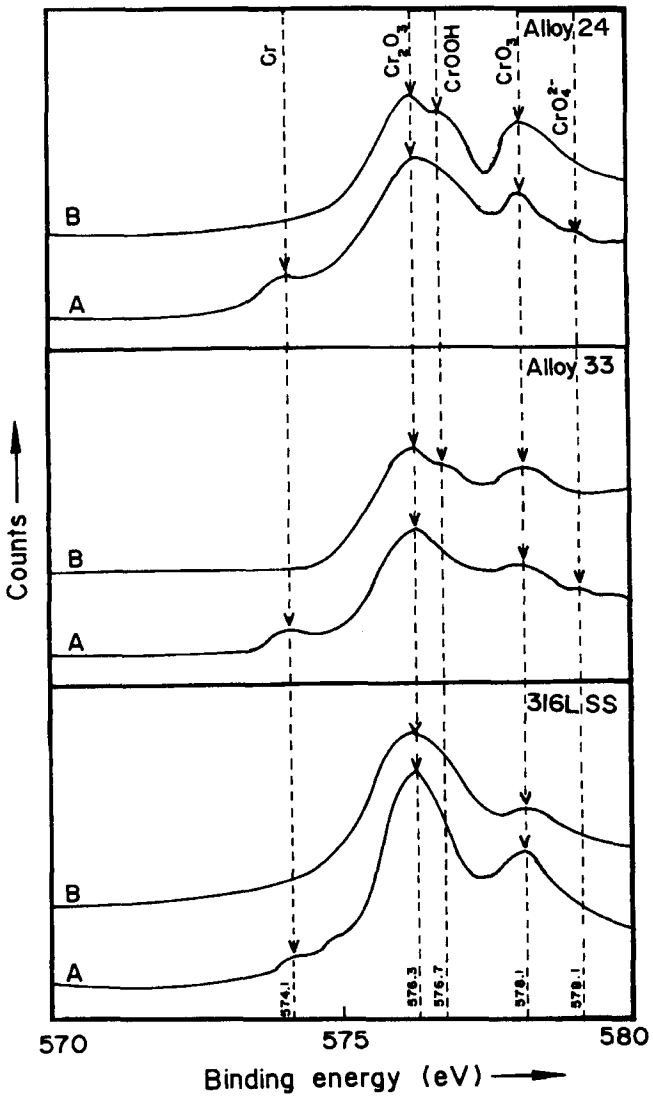

Fig. 3 XPS high-resolution spectra of chromium present in the films formed on alloy 24 (top), alloy 33, and type 316L SS (bottom). A, after sputtering; B, before sputtering

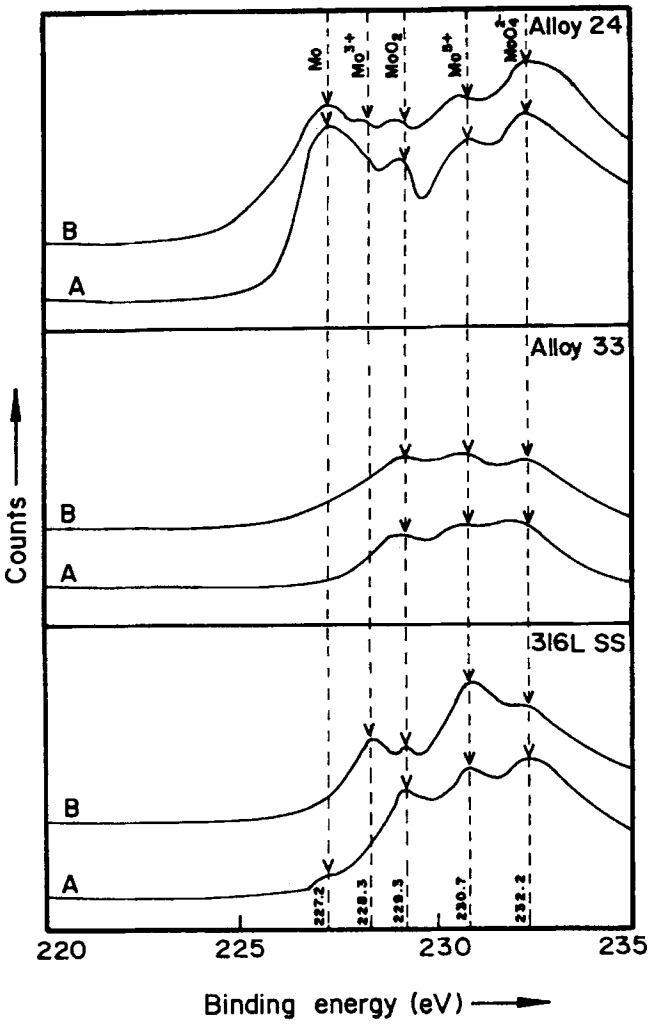

Fig. 4 XPS high-resolution spectra of molybdenum present in the films formed on alloy 24 (top), alloy 33, and type 316L SS (bottom). A, after sputtering; B, before sputtering

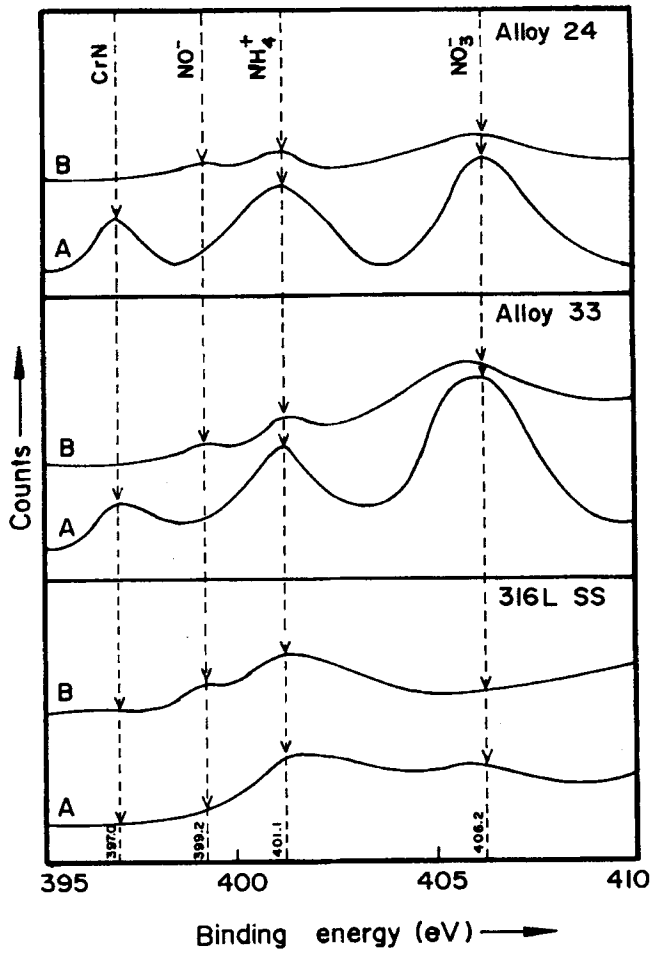

Fig. 5 XPS high-resolution spectra of nitrogen present in the films formed on alloy 24 (top), alloy 33, and type 316L SS (bottom). A, after sputtering; B, before sputtering

Comparing the binding energy values obtained for the recorded spectra with that of the reported values (Ref 14-17), the main peaks at 229.3 and 232.2 eV suggest the presence of molybdenum in the form of MoO_2 and MoO_4^{2-}.

3.3.3 Nitrogen (1*s*) Spectra

The specimens were scanned between 395.0 and 410.0 eV to obtain a clear picture of the chemical states of nitrogen in the passive film.

Nitrogen (1*s*) spectra of the type 316L sample showed the presence of nitrogen in binding energy values of 399.2 and 401.1 eV before sputtering. After sputtering the film, the peak at 406.2 eV was observed along with 399.2 and 401.1 eV (Fig. 5).

The high resolution spectra of nitrogen (1*s*) in the passive film of alloy 33 and alloy 24 revealed the peaks at 399.2, 401.1, and 406.2 eV at the outermost region of the passive film. After sputtering the passive film, the peak at 397.0 eV was observed along with 401.2 and 406.2 eV.

On the basis of the earlier reports (Ref 18-21), the peak located at 397.0 eV was determined to be caused by nitrogen incorporated in the passive film. Nitrogen present in the form of NO^-, NH_4^+, and NO_3^- with their corresponding binding energy values of 399.2, 402.0, and 406.2 eV showed a similar binding energy value when present in the passive film.

Hence, it appears as if nitrogen in the form of NO^- and NO_4^+ is present in the outer layer of alloy 33 and alloy 24. The inner layer consists of CrN, NH_4^+, and NO_3^- ions. The enrichment of CrN in these alloys would have impeded the release of metal ions through the outer layer and increased the resistance to pitting attack, whereas in the case of 316L SS, the peak at 397.0 eV was not observed, hence CrN was not found.

3.3.4 Chromium/Iron Peak Area Ratio

The chromium/iron peak area ratio is a vital parameter in deciding the stability of the passive film against leaching. The ability of an alloy to retard the leaching of chromium from the passive film indicates the resistance of the material toward localized corrosion attack. Swift et al. (Ref 21) indicated that the higher the chromium/iron peak area ratio, the higher the corrosion resistance.

The chromium/iron peak area ratios of the reference type 316L SS, alloy 33, and alloy 24 before and after sputtering are depicted in Fig. 6. From the results, it was observed that chro-

mium/iron peak area ratio was higher in the outer layer for all the alloys studied. After sputtering, the ratio was decreased.

Compared to type 316L, alloy 33 and alloy 24 showed a high chromium/iron peak area ratio and, hence the chromium content in the passive film of alloy 33 and alloy 24 was higher. This contributed to the higher corrosion resistance of these alloys compared to 316L SS.

3.4 *Effect of Alloying Elements in Improving the Passive Film Characteristics*

Compared to the reference type 316L SS, alloys 33 and 24 contain greater amounts of elements such as chromium and nitrogen; also, alloy 24 contains more molybdenum. The effect of chromium in improving the pitting corrosion resistance of the alloys has been dealt with in many studies (Ref 2, 3, 5). The chromium-rich passive film gets stabilized with the addition of the alloying elements and enhances the pitting potential of alloy 33 and alloy 24. From the XPS investigations, chromium is found to be enriched in the surface of alloy 33 and alloy 24, possibly in the form of CrOOH. Earlier reports suggest that the presence of CrOOH is beneficial in increasing the corrosion resistance as the hydroxide ions reduce the defects in the passive film. Hence, the presence of CrOOH with higher magnitude could have enhanced the corrosion resistance of alloy 33 and alloy 24. Moreover, chromium in the form of CrO_4^{2-} ions was also found to be beneficial as it is a potent passivating inhibitor (Ref 10), which resulted in enhanced corrosion resistance. However, in the case of 316L SS, the presence of CrOOH and CrO_4^{2-} was not identified.

The development of surface analysis techniques has enhanced knowledge of the passive layer structure and the role played by molybdenum (Ref 22, 23). Passive films formed in neutral and acid media consist of a rich chromium oxide inner layer (Cr_2O_3) and an outer layer containing hydrated chromium, iron, and molybdenum (Ref 24). For alloy 24, the increase in molybdenum to 4% increases the chromium concentration mainly of CrO_3 at the interface, thereby increasing the corrosion resistance of the alloy. This behavior is consistent with Sato's bilayer model (Ref 25) in which dehydration is favored by the change in film polarity. According to Hasimoto et al. (Ref 26), the passive film is inhomogeneous and contains a high density of microcracks through which current can leak. The microcracks are filled with water, and this is responsible for the high current.

The specific role of nitrogen in improving the stability of the passive film of stainless steels has been outlined by many investigators (Ref 18-21). The presence of nitrogen in the surface of the passive film in the form of elemental nitrogen and NH_4^+ was found in all three alloys.

During pit initiation, dissolution of nitrogen enriched at the metal/film interface forms NH_4^+ ions as:

$$[N] + 4\,H^+ + 3e^- \rightarrow NH_4^+$$

The formation of NH_4^+ at the initial stages of pitting aid in immediate repassivation of the pit surface by increasing the pH of the solution inside the pits. With the presence of higher amounts of nitrogen, 0.39%, alloy 33 and alloy 24 undergo dissolution at a faster rate, producing NH_4^+ at a higher concentration, which neutralizes the acidity within the localized sites, thereby increasing the corrosion resistance of the alloys.

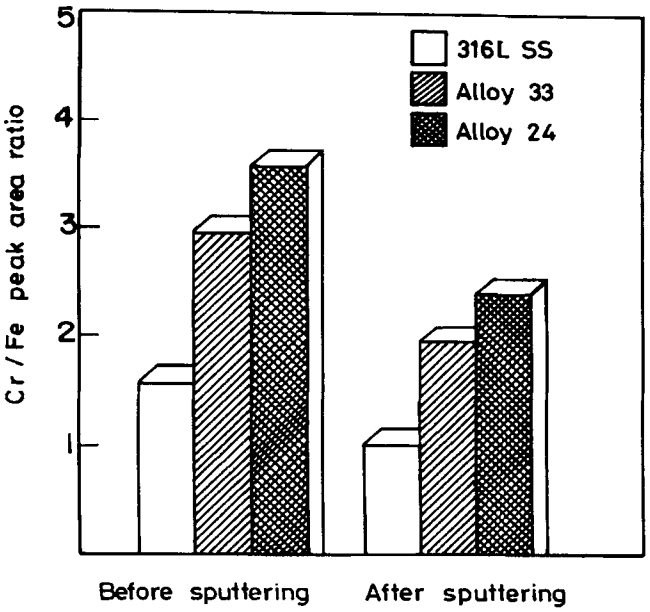

Fig. 6 Chromium/iron peak area ratio of the type 316L SS, alloy 33, and alloy 24 before and after sputtering of the passive film

From the XPS results, the presence of nitrates was observed for alloy 33 and alloy 24. The formation of nitrates in the case of alloy 33 and alloy 24 occurs by the following reactions:

$$NH_4^+ + H_2O \rightarrow NH_4OH + H^+$$

$$NH_4OH + H_2O \rightarrow NO_2^- + 7H^+ + 6e^-$$

$$NO_2^- + H_2O \rightarrow NO_3^- + 2H^+ + 2e^-$$

The beneficial effect of nitrates in inhibiting stainless steels are well known (Ref 27). NO_3^- is found to stabilize the passive film at a later stage of the repassivation process.

Other than NH_4^+ and NO_3^-, the presence of CrN cosegregation due to the incorporation of nitride with bulk chromium in the inner layers of alloy 33 and alloy 24 would have impeded the dissolution of metal ions through the passive film and increased the pitting corrosion resistance.

4. Conclusions

The new commercially available alloys, namely alloy 33 and alloy 24 have been studied with the objective of assessing the potential application of these alloys in marine environments. It was found that alloy 33 and alloy 24 were more noble than type 316L SS.

XPS studies showed the beneficial effect of alloying elements, that is, nitrogen, chromium, and molybdenum, in improving the stability of the passive film.

Acknowledgment

The authors would like to thank the VDM Corporation, USA, for providing the new alloys. The authors would also like to thank Dr. S.V. Narasimhan and Dr. Santhanu Bera, Scientific Officers, WSCL, IGCAR, Kalpakkam, India, for carrying out XPS investigations. G. Latha is grateful to the University Grants Commission, New Delhi, India, for financial assistance.

References

1. P.B. Lindsay, *Mater. Perform.*, Vol 25 (No. 12), 1986, p 13
2. A.J. Sedriks, *Corrosion*, Vol 45, 1989, p 510
3. G. Latha and S. Rajeswari, *J. Mater. Eng. Perform.*, Vol 5 (No. 5), 1996, p 577
4. N. Rajendran and S. Rajeswari, *J. Mater. Eng. Perform.*, Vol 5 (No. 1), 1996, p 46
5. N. Rajendran and S. Rajeswari, *J. Mater. Sci.*, Vol 31, 1996, p 6615
6. G. Latha and S. Rajeswari, *Corros. Prev. Control*, Vol 44 (No. 1), 1997, p 22
7. N. Rajendran, G. Latha, and S. Rajeswari, *Proceedings of the Fourth International Conference on Advances in Surface Engineering*, The Royal Society of Chemistry, 1996
8. B. Wallen, M. Liljas, and P. Stenvall, *Werkst. Korros.*, Vol 44, 1993, p 83
9. C.R. Clayton and Y.C. Lu, *J. Electrochem. Soc.*, Vol 133, 1986, p 2465
10. A.R. Brooks, C.R. Clayton, K. Doss, and Y.C. Lu, *J. Electrochem. Soc.*, Vol 133, 1986, p 2459
11. J. Olefjord, B. Brook, and V. Jelvestam, *J. Electrochem. Soc.*, Vol 132, 1985, p 2854
12. K. Sugimoto and Y. Sawada, *Corros. Sci.*, Vol 17, 1977, p 425
13. R.R. Sarmaitis and V.G. Rosousky, *Proceedings of the International Congress on Metallic Corrosion*, Vol 1, National Research Council of Canada, 1984, p 390
14. K. Asami, M. Naka, H. Hasimoto, and T. Masumoto, *J. Electrochem. Soc.*, Vol 127, 1980, p 2130
15. W.C. Moshier, G.D. Davis, J.S. Ahern, and H.F. Hough, *J. Electrochem. Soc.*, Vol 133, 1986, p 1063
16. W.C. Moshier, G.D. Davis, J.S. Ahern, and H.F. Hough, *J. Electrochem Soc.*, Vol 134, 1987, p 266
17. G. Latha, N. Rajendran, and S. Rajeswari, *Proceedings of the Fourth International Conference on Advances in Surface Engineering*, The Royal Society of Chemistry, 1996
18. I. Olefjord and B.O. Elfstrom, *Corrosion*, Vol 38, 1982, p 46
19. P. Marcus and M.E. Bussell, *Appl. Surf. Sci.*, Vol 59, 1992, p 7
20. A. Sadough Vanini, J.P. Audouard, and P. Marcus, *Corros. Sci.*, Vol 36, 1994, p 1825
21. A. Swift, A.G. Paul, and J.C. Vickerman, *Surf. Interface Anal.*, Vol 20, 1993, p 27
22. C.A. Olsson, *Corros. Sci.*, Vol 37 (No. 3), 1995, p 467
23. H.C. Brookes, J.W. Bayles, and F.J. Graham, *J. Appl. Electrochem.*, Vol 20, 1990, p 223
24. C.R. Clayton and Y.C. Lu, *J. Electrochem. Soc.*, Vol 133, 1986, p 2465
25. M. Sakashita and N. Sato, *Corros. Sci.*, Vol 27, 1987, p 473
26. K. Hasimoto, K. Asami, and K. Teramoto, *Corros. Sci.*, Vol 19, 1979, p 3
27. R.D. Willenbruch, C.R. Clayton, M. Oversluizen, D.Kim, and Y.C. Lu, *Corros. Sci.*, Vol 31, 1990, p 17